RESEARCH PAPER

A multilayered nanofibrous mucoadhesive system for chamomile and Lidocaine controlled delivery in aphthous

Zeynab Ahmadifard[1, 2], Nima Askarpour[1], Mohammad Hossein Abdani[1], Nooshin Tasharrofi[1, 2]*

[1] School of Pharmacy, Lorestan University of Medical Sciences, Khorramabad, Iran.
[2] Razi Herbal Medicines Research Center, Lorestan University of Medical Sciences, Khorramabad, Iran.

ABSTRACT

Objective(s): *The mucoadhesive systems are among the preferred dosage forms for oral disorders. They can be designed to concentrate the drug at the site of action, control the drug release, and reduce both the frequency of medication and the systemic side effects. This study aims to design and evaluate a multilayered oro-mucoadhesive film encompassing chamomile hydroalcoholic extract and Lidocaine to manage oral aphthous disorder.*

Materials and Methods: *A three-layer film for controlled release of Lidocaine and chamomile extract was prepared stepwise. The solvent casting method was used to prepare the fast-dissolving layer containing Lidocaine and chitosan/eudragit® S100 mucoadhesive layers. The middle layer, i.e. polycaprolactone nanofiber loaded with chamomile hydroalcoholic extract, was prepared by electrospinning. Layers were evaluated for appearance, thickness, pH, mucoadhesion, folding endurance, swellability, film disintegration time, content uniformity, chemical structure, and drug release. By attaching layers, the final system was prepared while DDSolver software was used to assess the release mechanism of Lidocaine and chamomile extract.*

Results: *The final dosage form had desirable physicochemical features, including mucoadhesive strength. The entire Lidocaine was released by diffusion over the first 4 hours, while the extract reached its maximum cumulative release (%) after about 24 hours under a combined release mechanism of diffusion and polymer relaxation.*

Conclusion: *Due to having polymers with different properties in each layer, our multilayered system allowed the controlled release of Lidocaine and chamomile extract, enabling it effectively used in the treatment of oral disorders.*

Keywords: *Matricaria recutita L. extract, Multilayer mucoadhesive device, Nanofiber, Buccal drug delivery, Aphthous stomatitis*

How to cite this article
Ahmadifard Z, Askarpour N, Abdani MH, Tasharrofi N. A multilayered nanofibrous mucoadhesive system for chamomile and Lidocaine controlled delivery in aphthous. Nanomed J. 2025; 12(2): 262-278. DOI: 10.22038/nmj.2025.78207.1912

INTRODUCTION

Aphthous stomatitis, or canker sore, is a common mouth disease that causes oral mucosa inflammation and pain [1]. Mouth ulcer treatments intend to lessen both discomfort and wound healing time and prevent disease recurrence [2]. Although systemic medications are commonly used [3], some impediments, such as adverse effects and poor control of oral plaque recurrence, exist [4, 5]. Thus, designing formulations with local and controlled drug delivery can provide a fertile ground for treatment [6, 7].

Anti-inflammatory and analgesic drugs and herbs are among the effective therapeutic agents for aphthous. For example, thanks to its actives (like azulene, chamazulene, and flavonoids) with anti-inflammatory, antispasmodic, antibacterial, antifungal, and analgesic properties, chamomile has shown beneficial effects in treating oral plaque discomfort and lesions [8, 9].

However, to effectively treat aphthous, a suitable drug delivery system is also required [10, 11]; as drug washing off with saliva and short residence time on site can overshadow the local treatments.

* *Corresponding Author Email: n_tasharrofi@yahoo.com*
Note. This manuscript was submitted on Febuary 19, 2024; approved on July 21, 2024

Mucoadhesive dosage forms paved the way to overcoming oral mucosal drug delivery obstacles; by localizing the articles at the affected sites, they can increase both the residence time and contact between the dosage form and the mucosa which helps high drug concentrations in the affected area. Minimizing systemic side effects as well as reducing the dose, and frequency of drug administration are among their other advantages [12-14].

Mucoadhesive systems are commonly made from polymers containing functional groups that can interact with mucosal components. For example, the presence of amine groups in chitosan made this polymer mucoadhesive as they can participate in hydrogen bonds as well as electrostatic interaction with negatively charged mucin moieties, such as sialic acid; Hydrophobic interactions are also considerable in chitosan mucoadhesion [15, 16]. Eudragit®s, polymethacrylate-based polymers with different functional groups, [17], and pectin are other examples of polymers with mucoadhesive properties. Pectin is a natural, biocompatible, and water-soluble polymer with good gelling and swelling properties; it is rich in carboxylic groups that can interact with mucin glycoproteins [18]. Enhancement in mucoadhesion can also be achieved through polymer combination [18-21].

In addition to mucoadhesion, to avoid patient discomfort, the ideal dosage form must possess other features like being soft and flexible, having a desirable thickness, withstanding mouth motions, and not excessively swelling. Unlike mucoadhesive tablets, the thin films are less bothersome in the mouth and do not interfere with the patient's eating or drinking [22]. Furthermore, by dressing the wound surface, films can reduce pain, and enhance the treatment efficacy.

Controlled drug release is another purpose for employing polymers in drug delivery systems [23]. Polymers provide a matrix in which the drug molecules are dispersed. Drugs can leave this medium by different mechanisms, like polymer degradation, swelling, or relaxation. For example, the slow biodegradation of water-insoluble polycaprolactone (PCL) polymer makes it suitable for sustained drug delivery [24].

There are different types of polymer matrices, including nanofibers. Having a high surface-to-weight ratio and porosity, nanofibers can effectively load and release the drugs; the simplicity and cost-effectiveness of their synthesis are among of other advantages. Again, the polymer type and loading method dictate the drug molecules' release pattern, i.e. immediate or modified release [25-27]. Since in controlled drug delivery systems polymers with limited water solubility are commonly used, their mucoadhesion capacity is low; So, augmenting them with mucoadhesive film, i.e. multilayered films, would likely be advantageous [1].

In the present study, we take advantage of mucoadhesion and limited biodegradation of polymers and develop a mucoadhesive dual-drug delivery system of chamomile and Lidocaine for the treatment of mouth ulcers; for this purpose, a tri-layered film was prepared as follows. The first layer was made of water-soluble polymers, i.e., pectin and HPMC K4M, to fast dissolve and release its payload, namely Lidocaine. The middle layer was the PCL nanofibers; the slow degradation of this polymer can extend the release of its loaded chamomile extract, our therapeutic agent. The third layer, composed of chitosan/Eudragit® S100, was considered for helping the mucoadhesiveness of the system. Each layer and final dosage form were characterized in terms of physicochemical properties and if necessary, improvements were made. By our system, Lidocaine could be rapidly released to exert its anesthetic effect for rapid pain relief while the release of chamomile extract occurs in a sustained manner.

MATERIAL AND METHODS

Material

High molecular weight Chitosan, pectin (from the citrus peel with galacturonic acid > 74%,) and polycaprolactone (PCL) (MW: 80,000 g/mol) were purchased from Sigma-Aldrich, Germany. Hydroxypropyl methylcellulose (HPMC) K4M was acquired from Alfa Aesar, United Kingdom. Eudragit® S100 [poly (methyl methacrylate-co-methacrylic acid)] was supplied from Evonik Industries, Germany. High molecular weight Polyvinyl alcohol (PVA), Propylene Glycol, Glycerol, acid citric, acid acetic, chloroform, acetone, ethanol, and agar were purchased from Merck, Germany. Hydroalcoholic extract of *Matricaria recutita L.* cv. Soroksari 40, acquired by percolation method, was a gift from Zarband Pharmaceuticals, Yasoj, Iran, in which apigenin-7-glucoside had a concentration of 0.9 mg/mL. Other reagents and chemicals were of the analytical grade.

Methods

Mucoadhesive layer preparation

Each layer of the system was separately prepared, and after evaluation, they were attached to make the final product.

Chitosan and Eudragit® S100 were used to prepare the mucoadhesive layer as follows; an exact amount of chitosan was dispersed in 7 ml of acetic acid 1% (V/V) at 70 °C and stirred until completely dissolved. The Eudragit® S100 was dissolved in a small amount of ethanol and then slowly added to the chitosan solution. The mixture was continuously stirred to obtain a homogeneous solution. Propylene glycol, and glycerol, as plasticizers, in a 3: 2 V/V ratio, were then added to the solution in appropriate amounts. The resultant solution was sonicated until the bubbles vanished, poured into a glass petri dish (diameter 7 cm), and dried in the oven at 40° C for 24 hours. The resulting film was kept in a desiccator in a sealed glass container. Various formulations of chitosan and Eudragit® S100 polymers with different concentrations of 1, 1.5, 2, and 3 % (W/V) of each and chitosan: Eudragit® S100 weight ratios of 1:1, 1:3, and 3:1 were prepared. Based on the results, the formulation containing 1.5% chitosan and 1.5% Eudragit® S100 (in a 1: 1 ratio) was chosen [28, 29].

Chamomile-extract loaded nanofiber layer fabrication

The nanofibrous layer laden with chamomile extract was constructed using electrospinning. The electrospinning solution was prepared by dissolving various amounts of PCL polymer in a 10 mL solvent mixture with a 1:1:3 volume ratio of chloroform, acetone, and ethanol, respectively, to make 8, 10, and 12 % W/V concentrations. The herbal extract in a final concentration of 2% (V/V) was added to the polymer solution; propylene glycol, 0.4 mL, was used as the co-solvent.

The nanofiber layer was produced by a standard and dual pump lab-scale electrospinning machine. The prepared polymer solution was injected using a 5 ml plastic syringe with a stainless steel needle (G22, 0.7 mm inner diameter, 32 mm lengths). A high-voltage source was used to apply the positive potential to the needle tip and the negative potential to the collector. The electrospinning parameters, namely the applied voltage, feed rate, and needle tip-to-collector distance, were adjusted to 17 kV, 1.6 mL /h, and 15 cm, respectively. The electrospinning process was performed at 25 °C and 45% relative humidity. The electrospun nanofibers were collected on aluminum foil covered on a spinning cylinder with a rotation speed of 300 rpm. The prepared nanofibers were then wrapped in aluminum foil and stored in a sealed container. The nanofiber layer without herbal extract was electrospun similarly and with the same parameters.

The morphology of PCL nanofibers

The morphology and diameter of PCL nanofibers were examined using a Field Emission Scanning Electron Microscope (FE-SEM) - (MIRA3 TESCAN - Czech Republic) at an acceleration voltage of 15 kV.

Uniformity of chamomile-extract content in the nanofiber layer

For evaluating the uniformity of chamomile extract content in the entire nanofibrous film, three pieces with a surface area of 1 cm^2 (11 cm) were cut from different parts of the extract-loaded and extract-free (as blank) nanofibers. The pieces were then completely dissolved in 3 mL of chloroform and the absorbance was measured at 254 nm (the absorbance peak of extract) by a UV spectrophotometer. As the extract contained 0.9 mg/mL apigenin-7-glucoside, the standard curve was prepared as “absorbance- equivalent apigenin-7-glucoside concentration (µg/mL)”, Fig. 2b; the obtained equation was used for concentration (µg/mL) and content (µg/ cm^2) measurements.

Synthesis of fast-dissolving film layer containing Lidocaine

The pectin and HPMC K4M were utilized as a fast-dissolving layer-forming polymer. Briefly, an exact amount of weighted pectin (in 0.5, 1, 2, 3, and 5% W/V final concentrations) dissolved in 7 mL of deionized water by magnet stirring. Following the dissolution, 0.5% (W/V) HPMC K4M or PVA polymer was added to the polymer solution. As a saliva-stimulating agent, Citric acid was added in a final concentration of 0.3% (w/v) and Lidocaine with a concentration of 1.8% (W/V). Propylene glycol and glycerol (in a 3:2 volume ratio) were used as plasticizers. The resulting homogenous solution was kept stationary to be a bubble-free solution and then poured into a glass

petri dish (7 cm in diameter) and dried in a 40 °C oven for 24 hours. The resulting film was stored in a sealed glass container. The drug-free film layer was prepared similarly to the drug-containing film method.

The film of 1% pectin and 0.5% HPMC K4M was chosen after primary evaluations.

Construction of the final formulation

The final formulation was a sandwich of as mentioned nanofibrous layer between mucoadhesive and fast-dissolving films. Briefly, following drying the films, one surface of the mucoadhesive film was wet with water vapor and then pressed and adhered to the electrospun layer. The fast-dissolving film layer was similarly attached to the electrospun nanofibers' other side [30]. A sealed glass container was used to store the multilayer mucoadhesive system's final formulation.

Characterization of the film layers

Each layer was subjected to the following tests based on its intended properties.

The physical appearance of film layers

The surface of the films should be uniform, flexible, and free of bubbles and wrinkles; these features were visually determined for each layer.

Weight uniformity

At least three pieces of each film with an area of 1 cm^2 were weighted by a digital scale (Mettler toledo, ME303, Switzerland); weight variations were then calculated.

Thickness measurement

The thickness should be uniform throughout the film; the thickness of three separated pieces, one in the center and two in the corners, of a film with a 1 cm^2 surface area was measured by a digital micrometer.

Folding endurance

Films must be flexible and not fracture when subjected to folding. The folding strength of the film was manually measured by folding it at a specific point until it was broken. The folding strength of a 1 cm^2 piece of film was calculated by successive folding and counting the number of folds.

Surface pH

The surface pH of the films was measured using an agar plate in the presence of artificial saliva [31, 32]. Artificial saliva was prepared with pH= 6.8. For this purpose, 1.2 g of potassium chloride, 0.85 g of sodium chloride, 0.05 g of magnesium chloride, 0.13 g of calcium chloride, and 0.13 g of di-potassium hydrogen orthophosphate were dissolved in distilled water using a magnetic stirrer. Then the solution was brought to a volume of one liter. The pH of the prepared saliva was adjusted to 6.8 [33, 34].

The agar gel was prepared by dissolving agar powder (1% w /v) in artificial saliva (pH 6.8) at 100 °C. The resulting solution was then put onto a petri dish, allowed to reach the ambient temperature, and gelled. Then, a 1 cm^2 piece of film was placed on the agar gel's surface, and the surface pH was measured after 10 minutes by placing pH indicator paper on the swollen film's surface.

Swellability study

The swelling of the films was also measured on the agar plate. Briefly, the initial weight of the 1 cm^2 films (W1) was determined, and then the samples were placed on the artificial saliva-moistened agar plate's surface. After ten minutes, excess water was withdrawn from the surface of the films with filter paper and the weight of the swelled films was measured (W2). The percentage of swellability of films was calculated using equation 1:

$$Swellability\ (\%) = \frac{W_2 - W_1}{W_1} \times 100$$

Equation (1)

Disintegration time

The disintegration time of the films was determined by immersing the film in 10 mL of artificial saliva (pH of 6.8) and stirring at 400 rpm speed and 37°C. When the film began to break, the disintegration time was visually recorded.

In vitro mucoadhesion strength study

The single-layered mucoadhesive layer and three-layered final film were tested for mucoadhesion. The mucoadhesive strength of the system was determined using a self-made and modified device, Fig. 1 [35]. Sodium alginate (10% w/v) was used as a mucosal model. As shown in Fig. 1, a piece of thread of appropriate and fixed

Fig. 1. The designated apparatus for measuring the mucoadhesive strength. Sodium alginate (10% W/V) was molded into a rectangular plate and wet with artificial saliva. The film was attached on one side to the sodium alginate and on the other side to a thread. A light container was attached to the end of the thread at a perpendicular angle. The water was dropwise added to the container until the film detached. Finally, the weight of the container and water was measured for mucoadhesive strength calculation.

length was attached to the surface of the chitosan/Eudragit® film (in the case of three layers, to the surface of the fast-dissolving layer), and the other end of the thread was attached to a light plastic cup (container). A glass roller was used to put this connection at a perpendicular angle. The film's surface was wet with artificial saliva, and the film was then put on the gel with a small force. The film was left there for two minutes to adhere to the gel. After releasing the container from the lab jack stage, water at a constant speed was instilled into the container with a micropipette until the film separated from the sodium alginate gel's surface. The weight of the container containing water was determined, and the film's mucoadhesive strength was calculated using Equation 2:

$$Mucoadhesive\ strength\ (N/cm^2) = \frac{W\,(Kg)\times g\,(^{m}/_{s^2})}{A\,(cm^2)}$$

Equation (2)

Where the *W* is the weight of the container plus the water, g is the acceleration of gravity (or 9.8 m/s^2) and A is the surface area of the films.

Uniformity of Lidocaine content in the fast-dissolving film layer

Three pieces of the Lidocaine-containing layer with a surface area of 1 cm^2 were cut from different parts of the film. The pieces were then put in a beaker containing 10 mL of artificial saliva (pH 6.8) and stirred at 200 rpm at 37 °C until completely dissolved. The concentration of Lidocaine was determined using the standard curve.

The calibration curve for Lidocaine was made by plotting absorbance (at 262 nm wavelength) against concentration, namely 25, 50, 100, 200, 400, 800, and 1000 µg/mL of Lidocaine in artificial saliva (pH= 6.8).

The Fourier Transform Infrared (FTIR) spectroscopic analysis

The attenuated total reflectance (ATR)-FTIR spectroscopy technique (using Thermo Nicolet ™ 4700 FT-IR Spectrometer), was employed for the chemical structure evaluation of films and extract. For this, the hydroalcoholic extract of chamomile first underwent rotary evaporation to remove its solvents, namely water and ethanol.

Powdered materials were first mixed with KBr and a pressed slab of them was used for FTIR. The spectrograms [transmittance (%) -wavenumber (Cm-1)] were acquired within the frequency range of 4000-400 Cm^{-1}.

X-ray diffraction (XRD) test

Molecules in solids can be positioned in different patterns and produce regular crystalline or amorphous structures. X-ray diffraction can reveal the solid structure. For evaluating the Lidocaine structure before and after embedding in the film, the XRD spectrum (using STOE Stadi P diffractometer) of Lidocaine powder, physical mixture of Lidocaine, HPMC, pectin and citric acid, and HPMC/pectin film containing Lidocaine was

acquired and diffractograms were compared.

In vitro drug release

For the drug release test, the final formulation was placed in a dialysis bag (cut off = 12 kDa), immersed in 10 mL of artificial saliva (pH of 6.8) at 37 °C, and agitated at 750 rpm. In defined intervals, the release medium (0.5 mL) was withdrawn and replaced with the same amount of artificial saliva. The concentration of Lidocaine and the herbal extract was determined using a UV spectrophotometer at 262 and 254 nm, respectively. The final system lacking Lidocaine in its fast-dissolving layer was used for the extract release test to reduce the Lidocaine and extract absorbance interference. The same approach was used for Lidocaine measurement, i.e., the nanofibrous layer without the extract was used here.

A drug-free three-layered formulation was utilized as a blank sample to more precisely evaluate the concentration of Lidocaine and herbal extract.

Mechanism of release kinetics

The mechanism of release kinetics of Lidocaine and herbal extract were evaluated using DDSolver (v 1.0; an Excel add-in software) software. The release data were fitted to various kinetic models, zero-order, first-order, and Higuchi as well as mechanism models, Makoid-Banakar, Korsmeyer-Peppas, Weibull, and Peppas-Sahlin models. The models with the highest adjusted- R2 and Model selection criterion (MSC) along with the lowest Akaike information criterion (AIC) values were considered the preferred drug release mechanisms.

Statistical analysis

All experiments were at least repeated three times, and the results were reported as mean ± SD. The ANOVA was used to compare groups by considering p-values ≤ 0.05 as statistically significant differences.

RESULTS

Optimization of polymer concentration in the mucoadhesive layer

Different concentrations (1, 1.5, 2, 3 % W/V) of chitosan and Eudragit® S100 polymers at different weight ratios were used to achieve a uniform mucoadhesive layer. The layers' transparency, smoothness, and flexibility were examined during polymer selection and concentration optimization. The best results were obtained with chitosan and Eudragit® S100 weight ratio of 1:1 and 1.5 % (W/V) concentration each; these levels of polymers were chosen for further experiments.

Optimization of polymer concentration in nanofiber layer

The electrospinning method was utilized to produce the PCL nanofiber layer. Several concentrations of PCL (8, 10, and 12 percent w/v) were utilized for electrospinning. Electrospun nanofibers made from 10% PCL showed no knots and a smooth surface. Therefore, this concentration was chosen for the final formulation.

Optimization of polymers in the fast-dissolving layer

Polymers with good water solubility are suitable for the fast-dissolving layer; pectin, HPMC K4M, and PVA were used to form the fast-dissolving layer. Small amounts of HPMC K4M or PVA were added to pectin to control the layer disintegration better. Different concentrations of pectin (0.5, 1, 2, 3, and 5% w/v) and constant concentrations of HPMC K4M or PVA (0.5% w/v) were utilized to make the film. The film containing 1% pectin combined with 0.5% HPMC K4M had better uniformity, smoothness, and flexibility.

Characterization of the layers and final formulation

Physical characteristics

All three layers and the final formulation have been evaluated for various physical properties, Table 1. The average weight, thickness, folding endurance, and surface pH were measured for all layers and the final product. Appropriate thickness is essential for patient comfort and acceptance; the oral film must also be flexible and tolerable to the mechanical pressures in the mouth. According to the folding endurance test, no cracks or fractures were seen by successive folding, which means the films are sufficiently flexible.

Mucoadhesive layer polymers must be able to draw ambient water over their fibers, allowing them to open and expose their reactive groups to mucosal reaction sites. Due to the hydrophilic polymers in the chitosan/eudragit® and pectin/HPMC K4M layers, they had a desirable and relatively high swelling value [36, 37], while the PCL

Table 1. Physical characteristics of the layers and final formulation

Layer	Weight uniformity	Thickness (µm)	Folding endurance	Surface pH	Swellability (%)	Mucoadhesion strength (N/cm^2)
Fast-dissolving	13.33±1.52	46.33±3.3	No cracks seen	7	242.55±25.57	-
Nanofiber	1.03±0.06	11.69 ± 0.5	No cracks seen	7	60.91±11.39	-
Mucoadhesive	11.33±1.5	26 ± 2.16	No cracks seen	6	250.66±26.77	1617.98±63.15
Final formulation	28.67±1.53	88.66±3.96	No cracks seen	7	-	1612.1± 17.67

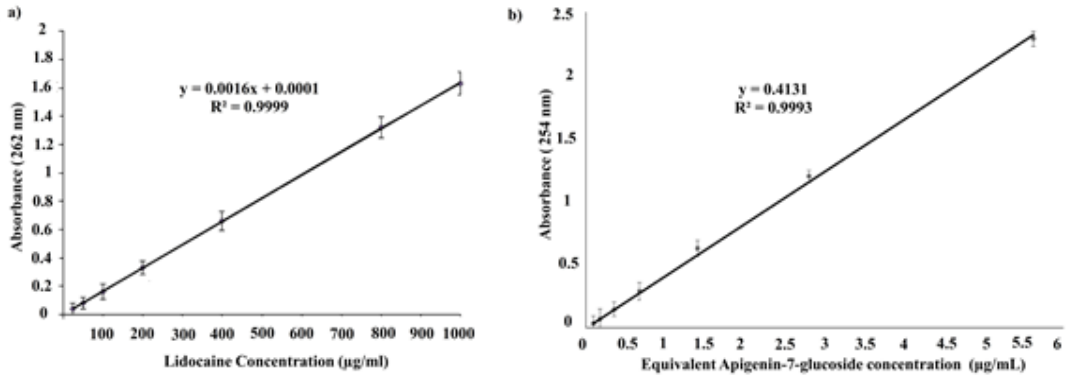

Fig. 2. Calibration curve of a) Lidocaine in artificial saliva (pH: 6.8) and b) chamomile extract. The extract had a maximum absorbance of 254 nm; as the concentration of apigenin-7-glucoside was 0.9 mg/mL of extract, the equivalent apigenin-7-glucoside concentration was calculated for each diluted sample.

layer did not swell as much as the two mentioned. The surface pH of all layers was in the range of saliva pH (approximately 5.6 to 7.4) and the buccal mucosa pH, which ensures no mucosal damage or irritation during use. The mucoadhesive layer also had enough mucoadhesion strength to hold the system on the mucosa.

Content uniformity of Lidocaine and disintegration time of fast dissolving layer

The fast-dissolving film's average Lidocaine content was 3484.79 ± 62.92 µg / cm^2, which indicates a narrow dose variation and evenly distribution of the drug throughout the film. The Lidocaine concentration was measured using its calibration curve, Fig. 2a.

The average disintegration time of the fast-dissolving film was 11.67 ± 1.53 minutes. This film took 61.66 ± 6.24 minutes to completely dissolve.

Morphology of PCL nanofibers

The morphology of PCL nanofiber was visualized by SEM. As shown in Fig. 3, the fabricated nanofibers have structural uniformity and desirable diameter sizes without knots.

Content uniformity of chamomile-extract in the nanofiber layer

Using the equation obtained from the chamomile extract standard curve, as shown in Fig. 2b, the equivalent apigenin-7-glucoside content was calculated to be 2.29, 1.71, and 2.13 µg/ cm^2 for cut pieces of nanofiber, with a mean of 2.04 µg/cm^2 0.24 SD.

FTIR analysis of films

FTIR is a useful method for the evaluation of chemical structures and interactions between materials.

Fig. 4a shows the FTIR spectrum of chamomile extract. The extract contains various phytochemicals like chamazulene, α-bisobolol, terpenoids, flavonoids (including apigenin, apigenin-7-glucoside, and luteolin), coumarins, and other actives that hold different functional groups like amine, hydroxyl, carboxyl, ester, alkene, aldehyde, and ketone. Accordingly, the wide peak of 3361 cm-1 is attributed to the phenolic O–H and amide N–H stretching. The jagged peak centered around 1606 cm-1 corresponds to the C=C and the C=O vibrations. The O-H bending of phenols, alcohols, and carboxyl groups resulted in a peak around 1393 cm-1. The band around 1277 cm^{-1} originates from the C-O and C-N stretching of esters and aromatic amines. The 1165 cm^{-1} could be attributed to the C–O group in terpenoids. The distinct broad band at 1035 cm^{-1} belongs to the C–O–C bond in aromatic ethers and

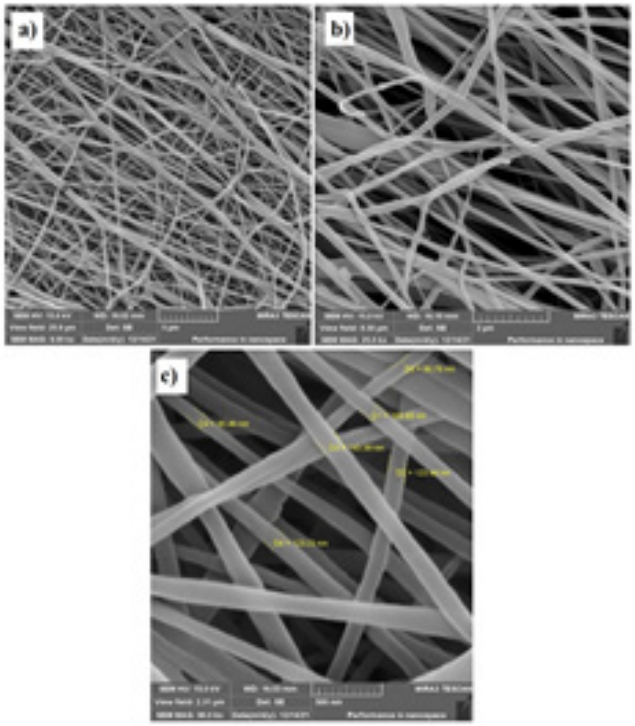

Fig. 3. SEM images of PCL nanofibers: with a scale bar of 5 µm (a), 2 µm (b), and 500 nm (c).

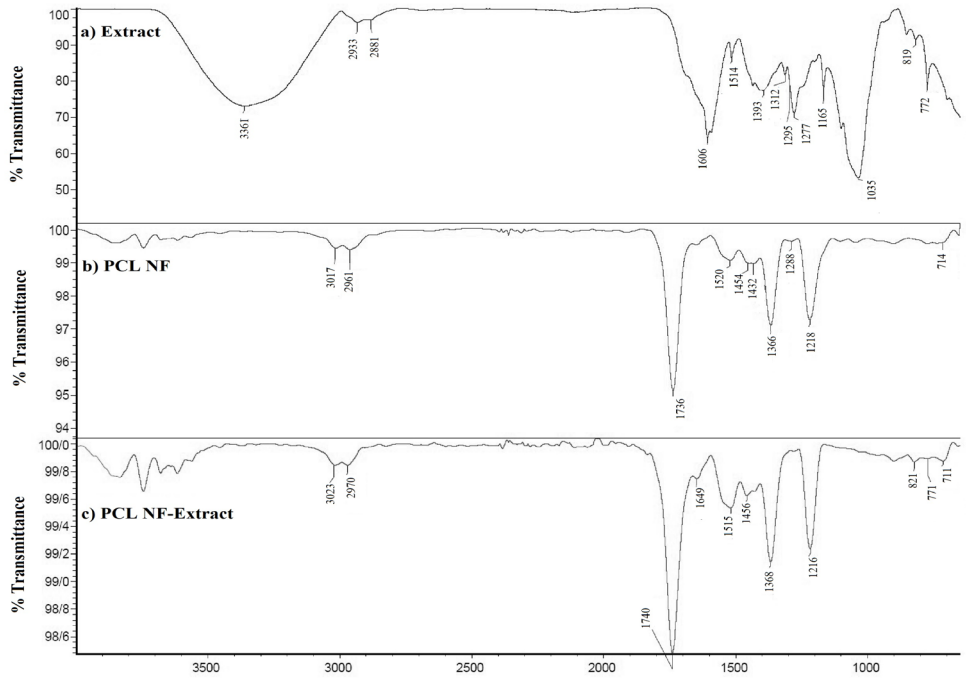

Fig. 4. The FTIR spectra of a) chamomile extract, b) polycaprolactone (PCL) nanofiber, and c) the chamomile extract loaded PCL nanofiber.

polysaccharides. [38].

Fig. 4b and Fig. 4c represent the ATR-FTIR spectra of the electrospun polycaprolactone (PCL) extract-free and extract-loaded PCL nanofibers, respectively. PCL is polyester and peaks related to C=O (1736 cm^{-1}), and C-O (1216 cm^{-1}) stretching can be seen in its spectrum.

It can be seen that the extract characteristic peaks are not evident in the PCL-extract nanofiber spectrum while PCL peaks are dominant, with no significant shift. This can be attributed to the low portion of extract in nanofibers which is superimposed with the PCL peaks and compatibility of extract and PCL.

The FTIR spectra related to the HPMC/pectin layer are shown in Fig. 5A. Fig. 5Ae shows the Lidocaine hydrochloride FTIR spectrum; the peaks of its main functional groups are seen at 3460 cm^{-1}, 3389 cm^{-1} (N-H stretching), 3190 cm^{-1} (C-H stretching of aromatic ring), 1658 cm-1 (C=O stretching), 1545 cm^{-1} (N-H deformation), 1477 cm^{-1} (aromatic C=C), and 1038 cm^{-1} (C-N stretching of amine). The majority of these peaks are covered by more intense peaks in the spectrum of HPMC/pectin film containing Lidocaine, Fig. 5Af. The film has a broad peak at 3319 cm^{-1} that belongs to the O-H group of pectin and HPMC polysaccharides. The C=O stretching of the carboxylic acid group of pectin is also seen at 1732 cm^{-1}. Peaks of 1683 cm^{-1} and 1541 cm^{-1} correspond to the C=O and N-H groups of Lidocaine, respectively, which are not seen in the spectrum of the film without the drug. The C=O band shift from 1658 cm^{-1} to 1683 cm^{-1} can be indicative of its participation in secondary interactions, like hydrogen bonds with O-H of polysaccharides. The shift of the O-H peak from 3449 cm^{-1} (which is seen in both HPMC and pectin spectra) to 3319 cm^{-1} can confirm their O-H hydrogen bonding.

The XRD evaluation

The Lidocaine structure in powdered form and after loading in the HPMC/pectin layer was evaluated by XRD. Fig. 5Ae indicates that Lidocaine had a crystalline structure prior to incorporating into the film, due to a diffraction pattern with distinctive peaks; its crystallinity was held when it was physically mixed with film ingredients, Fig. 5Bb. However, upon loading in the film, Lidocaine loses its crystallinity, Fig. 5Bc, which confirms its molecular dispersion in the film matrix.

In vitro release of Lidocaine and chamomile extract and determination of their release mechanisms

The release of Lidocaine and a chamomile hydroalcoholic extract from the mucoadhesive system was assessed in artificial saliva as the dissolution medium. The cumulative amount of released Lidocaine from the final formulation was more than 50% in the first half-hour, 87% at the end of 3 hours, and reached the maximum after 4 hours, Fig. 6a. It must be noted that, although the disintegration time of this layer is short, due to the attachment of hydrophobic PCL layer to this layer, its disintegration is delayed compared to the non-adhered fast-dissolving layer.

DDSolver software was applied for Lidocaine release mechanism evaluation; Zero-order, first-order, Higuchi, Makoid-Banakar, Korsmeyer-Peppas, Weibull, and Peppas-Sahlin models came to be analyzed for this purpose. The most fitted model was selected considering the highest R2-adjusted and MSC along with the lowest AIC; the results of the analysis are shown in Fig. 6b. The observed release results can also be compared with the predicted ones in each model by the software; the consistency of these can be seen in Fig. 6c.

About the chamomile extract, which was loaded in electrospun PCL polymer, less than 30% release was seen in the first four hours; after 18 hours, the amount of released extract was 81%, and after 24 hours, it reached almost 100%, Fig. 7a.

The results of release data analysis by DDSolver software are shown in Fig. 7b. The correlation between observed and predicted release data for each model is shown in Fig. 7c.

The contribution of diffusion (F) and polymer relaxation (R) in chamomile extract release from PCL nanofibers was evaluated by =

$$\frac{R}{F} = \frac{k_1}{k_2} t^m$$

equation, using parameters of the Peppas-Sahlin model [39], Fig. 7d.

DISCUSSION

Aphthous stomatitis is a common condition that affects the mouth's tissues; some challenges, like low residence time and rapid washout, can hinder its topical medication. Novel drug delivery systems can improve bioavailability, patient compliance, and precise medication. For

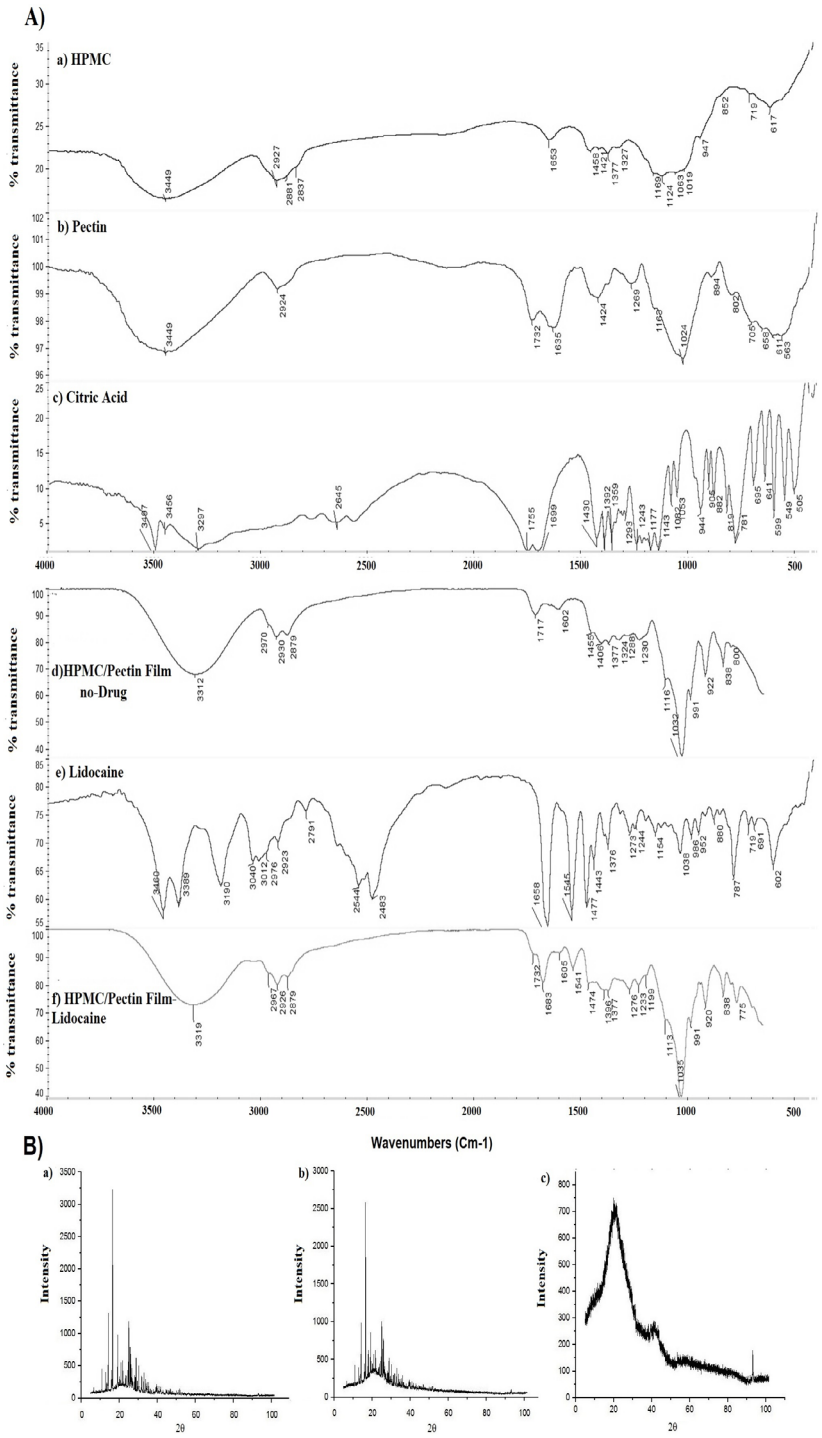

Fig. 5. HPMC/Pectin mucoadhesive layer evaluation by A) FTIR and B) X-ray diffraction. FTIR spectra belong to film components, i.e., a) HPMC polymer, b) Pectin, c) Citric acid, as well as d) the HPMC/Pectin film, e) Lidocaine HCl, and f) HPMC/Pectin containing Lidocaine. XRD diffractograms relate to a) Lidocaine HCl powder, b) a physical mixture of Lidocaine HCl, HPMC, Pectin, and Citric acid, and c) the HPMC/Pectin layer containing Lidocaine HCl.

a)

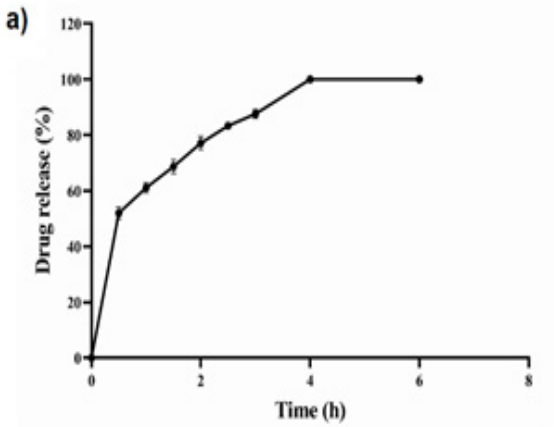

b)

Model	Equation*	Rate constant	Other parameters	Model parameters
Zero Order	$F=k_0 \times t$ $D_t = D_0 + k_0 t$	$k_0 = 31.36$		$R^2\_adj = 0.458$ AIC = 67.48 MSC = -0.71
First-Order	$F = 100\ (1-e^{-k_1 t})$	$k_1 = 0.884$		$R^2\_adj = 0.97$ AIC = 49.85 MSC = 1.48
Higuchi	$F=k_H \times t^{1/2}$	$k_H = 53.40$		$R^2\_adj = 0.94$ AIC = 48.76 MSC = 1.61
Makoid-Banakar	$F = k_{MB} t^n e^{-kt}$	$k_{MB} = 58.07$	$n = 0.21$ $k = 0.06$	$R^2\_adj = 0.99$ AIC = 15.69 MSC = 5.75
Korsmeyer-Peppas	$F = k_{KP} t^n$	$k_{KP} = 61.85$	$n = 0.32$	$R^2\_adj = 0.99$ AIC = 27.79 MSC = 4.24
Weibull	$F = 100\ (1 - e^{-\frac{t^\beta}{\alpha}})$		$\alpha = 0.994$ $\beta = 0.654$	$R^2\_adj = 0.97$ AIC = 42.40 MSC = 2.41
Peppas-Sahlin	$F = k_1 t^m + k_2 t^{2m}$	$k_1 = 42.60$ $k_2 = 19.15$	$m = 0.247$	$R^2\_adj = 0.99$ AIC = 27.96 MSC = 4.21

c)

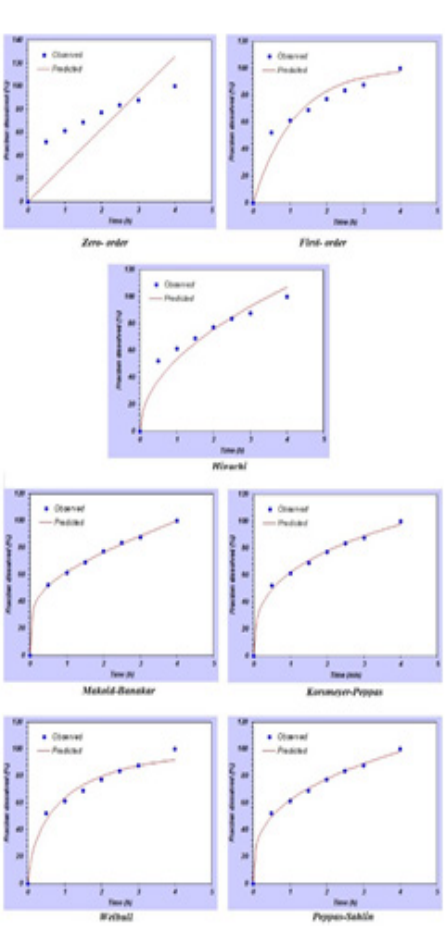

Fig. 6. The Lidocaine release evaluation. a) In vitro release profile of Lidocaine from the final system. b) the results of the release data analysis by DDSolver software for each model. c) the correlation between predicted and observed release data in different kinetics models. Excel 2013 was used for the release data graphing.

* F is the fraction of the drug that is released at the time t; n is exponent power; m is the Fickian diffusional coefficient; β is the shape factor and α is the scale factor.

a)

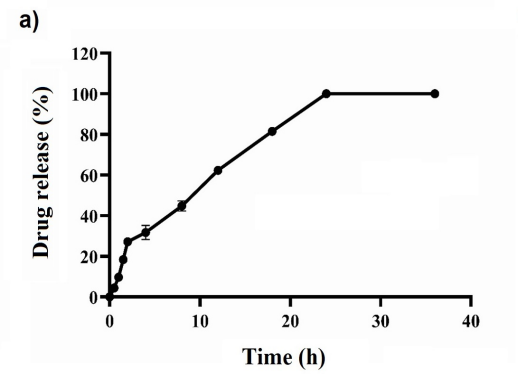

b)

Model	Equation*	Rate constant	Other parameters	Model parameters
Zero-Order	$F=k_0 \times t$ $D_t = D_0 + k_0 t$	k_0= 4.59		R^2_adj = 0.91 AIC = 69.91 MSC = 2.09
First-Order	$F= 100\ (1\text{-}e^{-k_1 t})$	k_1 = 0.094		R^2_adj =0.967 AIC = 60.04 MSC = 3.08
Higuchi	$F=k_H \times t^{1/2}$	k_H = 18.53		R^2_adj = 0.966 AIC = 60.69 MSC =3.01
Makoid- Banakar	$F = k_{MB} t^n e^{-kt}$	k_{MB} = 13.36	n= 0.59 k= -0.005	R^2_adj = 0.988 AIC = 51.12 MSC = 3.97
Korsmeyer-Peppas	$F = k_{KP} t^n$	k_{KP} = 12.73	n= 0.64	R^2_adj =0.989 AIC = 49.72 MSC = 4.11
Weibull	$F = 100\ (1 - e^{-\frac{t^\beta}{\alpha}})$		α = 9.49 β = 0.95	R^2_adj = 0.96 AIC = 61.80 MSC = 2.90
Peppas-Sahlin	$F= k_1 t^m + k_2 t^{2m}$	k_1= 12.80 k_2= 0.42	m= 0.58	R^2_adj = 0.988 AIC = 51.37 MSC = 3.94

c)

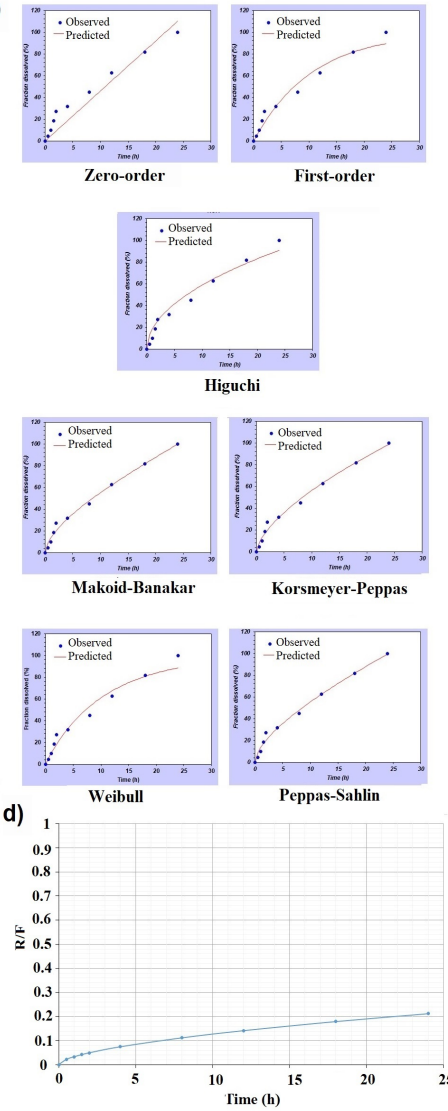

d)

Fig. 7. The chamomile extract release evaluation. a) In vitro release profile of chamomile extract from the final system. b) The calculated mechanism model parameters by analyzing release data through DDSolver software. c) The correlation between observed release data and predicted data in different kinetics models. d) The relative contribution of polymer relaxation (R) to diffusion (F) ratio in the drug release process with time

* F is the fraction of the drug that is released at the time t; n is exponent power; m is the Fickian diffusional coefficient; β is the shape factor and α is the scale factor.

example, due to hydration and interactions with mucus components, bioadhesive polymers in mucoadhesive systems can adhere to the mucosa and hold the dosage form in the intended location over a long period [40].

Besides, the drug release profile can be modified through careful polymer selection. For instance, hydrophilic polymers can be readily dissolved, which favors fast-dissolving formulations. On the other hand, less water-soluble polymers slow down drug release because of their low dissolution or degradation rate in an aqueous environment. A combination of polymers can also be used to create a multiphasic release profile and control drug release. For instance, in a study, a bilayer mucoadhesive film, composed of gellan gum and

hydroxyethylcellulose (HEC) layers, was prepared and loaded with moxifloxacin hydrochloride (Mox) and clove essential oil, respectively. Both layers have a biphasic release profile, with an initial burst followed by a sustained release. The immediate layer, or the HEC layer, disintegrated fast, releasing clove oil, but the sustained layer, i.e., gellan gum, swelled slowly, releasing Mox gradually [41].

In our study, we attempted to design and prepare a novel trilayered mucoadhesive system addressing oral aphthous by dual medication, i.e., Lidocaine and chamomile hydroalcoholic extract. We combined a variety of polymers with different characteristics and constructed a three-layer film composed of a mucoadhesive layer, a nanofiber layer containing plant extracts, and a fast-dissolving film layer loaded with an anesthetic agent, i.e., Lidocaine.

Water-soluble polymers like pectin, PVA, and HPMC K4M were selected for the fast-dissolving Lidocaine-loaded layer. Once placed on the surface, hydrophilic films attract water, followed by swell or disintegration. So, the included drug can be released at speeds dictated by the network's features [21]. The combination of pectin and HPMC K4M resulted in a desirable film with favored features.

Chitosan, along with Eudragit® S100, was used to produce the mucoadhesive layer. Compounds with carboxylic acid groups can adhere to the mucosa because, in their non-ionized state, they can form hydrogen bonds. Our data showed that the Chitosan/ Eudragit® S100 combination has proper bioadhesion, even compared to the "chitosan/alginate" film utilized in other studies [42, 43]. This high mucoadhesion could be due to amine groups on chitosan and undissociated carboxyl groups in Eudragit® S100, both of which can participate in hydrogen bonding and form higher and stronger bonds. Indeed, the application of Eudragit® S100 (poly (methyl methacrylate-methacrylic acid bearing free acidic groups) can boost the mucoadhesion strength along with chitosan [44, 45]. This feature made our system more acceptable than another trial in which eudragit® was not used, and the amount of chitosan was extremely high [46]. Swellability is another essential attribute of the mucoadhesive layer; thanks to the hydrophilic polymers in this layer, the swelling of chitosan / Eudragit® S100 was high enough.

PCL, a non-polar and water-insoluble polymer, nanofibers were recruited as the chamomile extract involving layer. PCL solution containing the extract was electrospun in the form of nanofibers. In general, the morphology of PCL fibers is substantially influenced by the viscosity and electrical conductivity of the spinning solutions as well as the polymer concentration. In the case of PCL, raising the solution concentration increases viscosity while lowering electrical conductivity, resulting in greater fiber diameter. Nodule formation was seen at concentrations less than 5% (W/V) of the polymer due to enhanced surface tension.

Two opposing views propose the effect of applied voltage on nanofiber diameter. First, the higher the applied voltage, the more material is drawn out of the needle tip, increasing the nanofiber diameter. The second logic implies that the higher the applied voltage, the greater the electrostatic force generated, reducing the diameter. The net result would be that no appreciable diameter change is observed in response to the applied voltage [47]. Because of the appropriate solution content (10% w/v), viscosity, and applied voltage (17 kV), the prepared nanofibers had no knots and were smaller than 150 nm in diameter [25].

Another main parameter is the flow rate of the polymer solution inside the syringe. Lower flow rates are generally preferred because the polymer solution will have sufficient polarization time. Because of the short drying time before reaching the collector and the low tensile stresses, thick-diameter bead fibers form instead of smooth, thin-diameter fibers when the flow rate is too high. The distance between the collector and the syringe tip has also been shown to impact fiber diameter and morphology. That is to say, if the distance between the needle and the collector is too short, the fiber will not have enough time to solidify before reaching the collector, and if the distance is too long, a bead fiber will result. Solvent-induced dryness is generally known as one of the electrospun fibers' most essential physical features; hence, the optimal distance is advised. As it aimed to reduce the diameter of PCL nanofibers, the distance between the needle and the collector in this investigation was chosen at 15 cm. However, in similar studies, the distance was less than 10 cm [26, 48]. Therefore, the diameter of PCL nanofibers was significantly reduced due to the increased distance gap between the needle

and the collector.

The compatibility and secondary interactions between drug and formulation components are of other important properties since they can affect the drug's release, stability, and efficacy. For instance, the ester group in PCL, the hydroxyl group of polysaccharides (HPMC and pectin), and the amid group in Lidocaine can participate in hydrogen bonding or carboxylate anion in pectin can electrostatically interact with cations, like protonated amines. FTIR technique allows for the identification of possible interactions between materials along with chemical structure. FTIR spectra of films showed insignificant interaction, except for hydrogen bonds, between chamomile extract or Lidocaine with their film-forming polymers. Moreover, XRD diffractograms proved that lidocaine dispersed molecularly in the film. These findings confirm the compatibility of these actives with formulation components, which can also lead to drug release independent of intermolecular interactions.

The drug release was studied for our final system as well. Although two drugs were embedded in our system, we intended to schedule their release; i.e., due to the ready disintegration of the pectin/HPMC K4M, the rapid release of Lidocaine was expected, whereas PCL nanofibers extended the chamomile extract exit. Our results showed that more than 50% of the cumulative amount of lidocaine was released in the first half hour. In a study that used Carbopol 940 and Poloxamer 407 polymers for buccal administration of Lidocaine, nearly 80% of the loaded Lidocaine was released in the first half-hour, which is mainly related to the solubility of the polymers [49].

Based on our results, Lidocaine could reach its maximum 80 % cumulative after about four hours.

Compared to the current study, a mucoadhesive system composed of chitosan and HPMC polymers showed no superiority in releasing Lidocaine in the first half-hour. This system could release 80% of Lidocaine after 4 hours, while our system could release the same amount in the third hour [50].

Drug diffusion and polymer swelling and degradation are common phenomena in drug release from matrices. The diffusion or Fickian release can occur under zero-order, first-order, and Higuchi kinetics. Each model equation includes the rate constant along with other parameters; the rate constant indicates how rapidly a reaction occurs.

Other involved mechanisms can be revealed through mechanism models, like the Korsmeyer-Peppas model. The Korsmeyer-Peppas equation is defined as $Mt/M\infty=ktn$, where $Mt/M\infty$ is the % cumulative drug released at time t, K is the kinetic constant, and n is the release exponent, which defines the mechanism. If n= 0.5 the diffusion controls the drug release (case I), when the n= 1 the swelling is the main phenomenon in drug release (non-Fickian or case II), in the case of $0.5<n<1$, both diffusion and swelling participate in drug release (anomalous), and if n is more than 1, it indicates an increase in concentration gradient over time and deviation from the linear profile [39, 51].

According to DDSolver analysis, the first-order mechanism (concentration-dependent release) governs Lidocaine diffusion. The hydrophilic nature of the matrix of this layer permits the penetration of the medium, and the prompt release of Lidocaine (water-soluble drug), i.e., the rate of solvent transport is much higher than polymer relaxation. Although the high R2-adjusted in the Higuchi model is considerable. The involvement of both mechanisms might be due to the fast disintegration of this layer and the readily movement of the drug in the matrix which fades the role of the drug-depleted section (which is seen in the Higuchi model) in drug release.

High R2-adjusted in all mechanism-based models (Makoid-Banakar, Korsmeyer-Peppas, Weibull, and Peppas-Sahlin) makes them suitable for data interpretation. The n= 0.21 in Makoid-Banakar (which is less than 0.5), n= 0.32 in the Korsmeyer-Peppas model (which is less than 0.5), and β= 0.645 in the Weibull model (which is less than 0.75) confirm the Fickian release of the Lidocaine.

On the other hand, the release kinetics of chamomile hydroalcoholic extract from PCL was according to the Higuchi model; the Higuchi mechanism is commonly seen in matrix systems in which the pathway increases as the drug leaves the system. As the PCL does not decompose in the aqueous medium, the surface of the polymer is emptied of the drug over time, and the distance in the polymer changes and becomes longer, so the release kinetics will be according to Higuchi's.

PCL is a water-insoluble polymer that is not disintegrated in aqueous media and as reported in Table 1, its swelling was about 61%, so, the drug diffusion and polymer swelling can govern the

drug release.

By analyzing the release data using DDSolver software, Fig. 7b, 0.5<n<1 in Makoin-Banakar and Korsmeyer-Peppas, and 0.75< <1 in Weibull confirmed the role of the diffusion and swelling in the drug release.

Based on the Peppas-Sahlin model parameters, the role of the polymer relaxation (R) and diffusion (F) can be calculated by = [39]. According to Fig. 7d, diffusion is the predominant mechanism in drug release; the relatively low swellability of the nanofiber layer (about 61%) can confirm this.

This insoluble polymeric base made chamomile extract release slowly over 24 h; within the first 4 hours, less than 30% of the chamomile extract was released from the electrospun PCL polymer; at the end of 18 hours, the % cumulative amount reached 81%, and after 24 hours, it was almost 100%. In a study, higher concentrations of PCL (2-fold) and auxiliary polymers, chitosan, and PVA, were used; 50% of the extract was released from the system within 24 hours [52]. As the PCL is a hydrophobic polymer with slow biodegradability, the release is expected to slow down as the polymer concentration increases.

Chamomile hydroalcoholic extract-loaded PCL (20% w/v) nanofibers were prepared in another study. Because PCL is an amorphous polymer and chamomile was present on the fiber surfaces, the extract had a burst and fast release before 10 h [52, 53]. However in our research, as the PCL layer is entrapped within two other layers of films and the chamomile should have diffused through the first layer, the initial burst release was not significant. As a result, the release was more gradual than the mentioned above system. Consequently, in the currently developed mucoadhesive system, Lidocaine begins to release first, following the slow release of the hydroalcoholic extract of chamomile, which has a soothing and possibly therapeutic effect on the oral plague. This release pattern and appropriate mucoadhesion strength of our system make it a suitable sustain-release drug delivery system that can be prescribed once a day.

CONCLUSION

This study aimed to design an effective oral mucoadhesive system for dual drug delivery to oral plaque. To fulfill this purpose, a three-layer system consisting of Lidocaine-containing pectin/HPLC film, chamomile extract-loaded PCL nanofiber, and chitosan/eudragit® mucoadhesive film was synthesized and characterized. The developed system had suitable physicochemical features, including mucoadhesive strength, and showed compatibility between ingredients. Lidocaine and chamomile extract were released effectively using this system; i.e., in the first three hours, more than 85 % of the Lidocaine, and by the end of the 24 hours, the loaded chamomile extract was released from the system. Through this system, we could introduce an efficient dosage form with controlled drug release, which can be effectively used for drug delivery to oral plaque as well as other oral diseases. Even though more studies are needed, especially in vivo tests, we are currently through. Besides, the effective antibacterial and antifungal concentration of chamomile extract must be determined to define the required dose in this system.

DATA AVAILABILITY

The data that this study generated or analyzed can be accessed from the corresponding author, upon a valid request.

FUNDING

The preparation of this manuscript did not receive any funding.

ETHICAL APPROVAL

This study has received the Ethics Code of IR.LUMS.REC.1400.148 from the Ethics Committee of Lorestan University of Medical Sciences.

CONFLICTS OF INTEREST

The authors all confirm that they have no conflict of interest.

REFERENCES

1. Wei L, Wu S, Shi W, Aldrich AL, Kielian T, Carlson MA, et al. Large-scale and rapid preparation of nanofibrous meshes and their application for drug-loaded multilayer mucoadhesive patch fabrication for mouth ulcer treatment. ACS Appl Mater Interfaces. 2019;11(32):28740-28751.
2. Suter VGA, Sjolund S, Bornstein MM. Effect of laser on pain relief and wound healing of recurrent aphthous stomatitis: a systematic review. Lasers Med Sci. 2017;32(4):953-963.
3. Sharma D, Garg R. A comprehensive review on aphthous stomatitis, its types, management and treatment available. J Dev Drugs. 2018;7(2):1-8.
4. Halboub E, Al-Maweri SA, Parveen S, Al-Wesabi M, Al-Sharani HM, Al-Sharani A, et al. Zinc

supplementation for prevention and management of recurrent aphthous stomatitis: a systematic review. J Trace Elem Med Biol. 2021;68:126811.
5. Al-Maweri SA, Halboub E, Ashraf S, Alqutaibi AY, Qaid NM, Yahya K, et al. Single application of topical doxycycline in management of recurrent aphthous stomatitis: a systematic review and meta-analysis of the available evidence. BMC Oral Health. 2020;20:1-8.
6. Arany P. Craniofacial wound healing with photobiomodulation therapy: new insights and current challenges. J Dent Res. 2016;95(9):977-984.
7. Zhang C, Liu Y, Li W, Gao P, Xiang D, Ren X, et al. Mucoadhesive buccal film containing ornidazole and dexamethasone for oral ulcers: in vitro and in vivo studies. Pharm Dev Technol. 2019;24(1):118-126.
8. Li CL, Huang HL, Wang WC, Hua H. Efficacy and safety of topical herbal medicine treatment on recurrent aphthous stomatitis: a systemic review. Drug Des Devel Ther. 2016;10:107-115.
9. Rezvaninejad R, Nabavi N, Khoshroo SM, Torabi N, Atai Z. Herbal Medicine in Treatment of Recurrent Aphthous Stomatitis: A Literature Review. J Iran Dent Assoc. 2017;29(3):127-134.
10. Sah A, Naseef PP, Kuruniyan MS, Jain GK, Zakir F, Aggarwal G. A comprehensive study of therapeutic applications of chamomile. Pharmaceuticals. 2022;15(10):1284.
11. Kani VT, Bharathwaj V, Nimmy P, Sindhu R, Dhamodhar D, Sathiapriya S, et al. Therapeutic effects of Chamomilla extract in oral diseases-A Systematic Review. J Adv Med Dent Scie Res. 2023;11(4):50-55.
12. Mamatha K, Venkatesh P. A review on: mucoadhesive drug delivery systems. J Innov Appl Pharm Sci. 2022:32-36.
13. Wang T, Fleming E, Luo Y. An overview of the biochemistry, synthesis, modification, and evaluation of mucoadhesive polymeric nanoparticles for oral delivery of bioactive compounds. Adv Compos Hybrid Mater. 2023;6(1):6.
14. Joshi R, Akram W, Chauhan R, Garud N. Thin Films: A Promising Approach for Drug Delivery System. Drug Carriers: IntechOpen. 2022.
15. TM MW, Lau WM, Khutoryanskiy VV. Chitosan and Its Derivatives for Application in Mucoadhesive Drug Delivery Systems. Polymers (Basel). 2018;10(3):267.
16. Yermak IM, Davydova VN, Volod'ko AV. Mucoadhesive marine polysaccharides. Mar Drugs. 2022;20(8):522.
17. Nikam A, Sahoo PR, Musale S, Pagar RR, Paiva-Santos AC, Giram PS. A systematic overview of Eudragit® based copolymer for smart healthcare. Pharmaceutics. 2023;15(2):587.
18. Szekalska M, Czajkowska-Kośnik A, Maciejewski B, Misztalewska-Turkowicz I, Wilczewska AZ, Bernatoniene J, et al. Mucoadhesive alginate/pectin films crosslinked by calcium carbonate as carriers of a model antifungal drug—Posaconazole. Pharmaceutics. 2023;15(10):2415.
19. Villanova J, Ayres E, Oréfice R. Design, characterization and preliminary in vitro evaluation of a mucoadhesive polymer based on modified pectin and acrylic monomers with potential use as a pharmaceutical excipient. Carbohydr Polym. 2015;121:372-81.
20. Jantrawut P, Chaiwarit T, Jantanasakulwong K, Brachais CH, Chambin O. Effect of Plasticizer Type on Tensile Property and In Vitro Indomethacin Release of Thin Films Based on Low-Methoxyl Pectin. Polymers (Basel). 2017;9(7):289.
21. Fernandes FP, Fortes AC, da Cruz Fonseca SG, Breitkreutz J, Ferraz HG. Manufacture and characterization of mucoadhesive buccal films based on pectin and gellan gum containing triamcinolone acetonide. Int J Polym Sci. 2018;2018.
22. Jacob S, Nair AB, Boddu SH, Gorain B, Sreeharsha N, Shah J. An updated overview of the emerging role of patch and film-based buccal delivery systems. Pharmaceutics. 2021;13(8):1206.
23. Sung YK, Kim SW. Recent advances in polymeric drug delivery systems. Biomater Res. 2020;24(1):12.
24. Mohamed RM, Yusoh K. A review on the recent research of polycaprolactone (PCL). Adv Mat Res. 2016;1134:249-255.
25. Potrč T, Baumgartner S, Roškar R, Planinšek O, Lavrič Z, Kristl J, et al. Electrospun polycaprolactone nanofibers as a potential oromucosal delivery system for poorly water-soluble drugs. Eur J Pharm Sci. 2015;75:101-113.
26. Adhikari U, An X, Rijal N, Hopkins T, Khanal S, Chavez T, et al. Embedding magnesium metallic particles in polycaprolactone nanofiber mesh improves applicability for biomedical applications. Acta Biomater. 2019;98:215-234.
27. Shan W, Zhu X, Liu M, Li L, Zhong J, Sun W, et al. Overcoming the diffusion barrier of mucus and absorption barrier of epithelium by self-assembled nanoparticles for oral delivery of insulin. ACS Nano. 2015;9(3):2345-2356.
28. Kouchak M, Handali S, Naseri Boroujeni B. Evaluation of the Mechanical Properties and Drug Permeability of Chitosan/Eudragit RL Composite Film. Osong Public Health Res Perspect. 2015;6(1):14-19.
29. Sardou HS, Akhgari A, Garekani HA, Sadeghi F. Screening of different polysaccharides in a composite film based on Eudragit RS for subsequent use as a coating for delivery of 5-ASA to colon. Int J Pharm. 2019;568:118527.
30. Mašek J, Lubasova D, Lukáč R, Turanek-Knotigova P, Kulich P, Plockova J, et al. Multi-layered nanofibrous mucoadhesive films for buccal and sublingual administration of drug-delivery and vaccination nanoparticles-important step towards effective mucosal vaccines. J Control Release. 2017;249:183-

195.
31. Jelvehgari M, Montazam SH, Soltani S, Azar K, Montazam SA. Fast dissolving oral thin film drug delivery systems consist of ergotamine tartrate and caffeine anhydrous. Pharm Sci. 2015;21(2):102-10.
32. Begum MY, Alqahtani A, Ghazwani M, Ramakrishna M, Hani U, Atiya A, et al. Preparation of Carbopol 934 based ketorolac tromethamine buccal mucoadhesive film: in vitro, ex vivo, and in vivo assessments. Int J Polym Sci. 2021;2021(1):4786488.
33. Paczkowska-Walendowska M, Szymanowska D, Cielecka-Piontek J. Mechanochemical Properties of Mucoadhesive Tablets Based on PVP/HPβCD Electrospun Nanofibers as Local Delivery of Polygoni Cuspidati Extract for Treating Oral Infections. Pharmaceuticals. 2023;16(4):579.
34. Nowakowska-Toporowska A, Malecka K, Raszewski Z, Wieckiewicz W. Changes in hardness of addition-polymerizing silicone-resilient denture liners after storage in artificial saliva. J Prosthet Dent. 2019;121(2):317-321.
35. Akbari J, Saeedi M, MortezaSemnani K, Ameri M. The effect of type and amount of polymer on the bioadhesive properties and drug release of diclofenac sodium buccoadhesive films. J Mazandaran Univ Med Sci. 2014;24(113):92-103.
36. Bruschi ML, de Souza Ferreira SB, da Silva JB. Mucoadhesive and mucus-penetrating polymers for drug delivery. Nanotech Oral Drug Deliv: Elsevier. 2020;77-141.
37. Kumar A, Naik PK, Pradhan D, Ghosh G, Rath G. Mucoadhesive formulations: Innovations, merits, drawbacks, and future outlook. Pharm Dev Technol. 2020;25(7):797-814.
38. Parlinska-Wojtan M, Kus-Liskiewicz M, Depciuch J, Sadik O. Green synthesis and antibacterial effects of aqueous colloidal solutions of silver nanoparticles using camomile terpenoids as a combined reducing and capping agent. Bioprocess Biosyst Eng. 2016;39:1213-1223.
39. Bruschi ML. Strategies to modify the drug release from pharmaceutical systems: Woodhead Publishing; 2015.
40. Alawdi S, Solanki AB. Mucoadhesive drug delivery systems: A review of recent developments. J Sci Res Med Biol Sci. 2021;2(1):50-64.
41. Li A, Khan IN, Khan IU, Yousaf AM, Shahzad Y. Gellan Gum-Based Bilayer Mucoadhesive Films Loaded with Moxifloxacin Hydrochloride and Clove Oil for Possible Treatment of Periodontitis. Drug Des Devel Ther. 2021;15:3937-3952.
42. Gilhotra RM, Mishra DN. Alginate-chitosan film for ocular drug delivery: effect of surface cross-linking on film properties and characterization. Pharmazie. 2008;63(8):576-579.
43. Lefnaoui S, Moulai-Mostefa N, Yahoum MM, Gasmi SN. Design of antihistaminic transdermal films based on alginate–chitosan polyelectrolyte complexes: characterization and permeation studies. Drug Dev Ind Pharm. 2018;44(3):432-443.
44. Vasantha PV, Puratchikody A, Mathew ST, Balaraman AK. Development and characterization of Eudragit based mucoadhesive buccal patches of salbutamol sulfate. Saudi Pharm J. 2011;19(4):207-214.
45. Cazorla-Luna R, Martín-Illana A, Notario-Pérez F, Bedoya LM, Tamayo A, Ruiz-Caro R, et al. Vaginal polyelectrolyte layer-by-layer films based on chitosan derivatives and Eudragit® S100 for pH responsive release of tenofovir. Mar drugs. 2020;18(1):44.
46. Koland M, Charyulu RN, Vijayanarayana K, Prabhu P. In vitro and in vivo evaluation of chitosan buccal films of ondansetron hydrochloride. Int J Pharm Investig. 2011;1(3):164-171.
47. Kolbuk D, Guimond-Lischer S, Sajkiewicz P, Maniura-Weber K, Fortunato G. The effect of selected electrospinning parameters on molecular structure of polycaprolactone nanofibers. Int J Polym Mater Polym Biomater. 2015;64(7):365-377.
48. Chinnappan BA, Krishnaswamy M, Xu H, Hoque ME. Electrospinning of biomedical nanofibers/ nanomembranes: effects of process parameters. Polymers. 2022;14(18):3719.
49. Cavallari C, Fini A, Ospitali F. Mucoadhesive multiparticulate patch for the intrabuccal controlled delivery of lidocaine. Eur J Pharm Biopharm. 2013;83(3):405-414.
50. Pleguezuelos-Villa M, Nacher A, Hernandez MJ, Buso M, Barrachina M, Penalver N, et al. A novel lidocaine hydrochloride mucoadhesive films for periodontal diseases. J Mater Sci Mater Med. 2019;30(1):14.
51. Talevi A, Ruiz ME. Korsmeyer-Peppas, Peppas-Sahlin, and Brazel-Peppas: Models of Drug Release. The ADME Encyclopedia: A Comprehensive Guide on Biopharmacy and Pharmacokinetic. Cham: Springer International Publishing. 2022; 613-621.
52. Shokrollahi M, Bahrami SH, Nazarpak MH, Solouk A. Multilayer nanofibrous patch comprising chamomile loaded carboxyethyl chitosan/poly (vinyl alcohol) and polycaprolactone as a potential wound dressing. Int J Biol Macromol. 2020;147:547-559.
53. Motealleh B, Zahedi P, Rezaeian I, Moghimi M, Abdolghaffari AH, Zarandi MA. Morphology, drug release, antibacterial, cell proliferation, and histology studies of chamomile-loaded wound dressing mats based on electrospun nanofibrous poly(varepsilon-caprolactone)/polystyrene blends. J Biomed Mater Res B Appl Biomater. 2014;102(5):977-987.